

- [10] K. A. Ingebritsen *et al.*, "A Schottky diode acoustic memory and correlator," *Appl. Phys. Lett.*, vol. 26, pp. 596-598, 1975.
- [11] C. Maerfelt and Ph. Defranould, "A surface wave memory device using pn diodes," in *IEEE Ultrasonics Symp. Proc.*, pp. 209-211, 1975.
- [12] H. C. Tuan *et al.*, "A new zinc oxide on silicon monolithic storage correlator," in *IEEE Ultrasonics Symp. Proc.*, pp. 496-499, 1977.
- [13] H. C. Tuan, J. E. Bowers, and G. S. Kino, "Theoretical and experimental results for monolithic SAW memory correlators," *IEEE Trans. Sonics Ultrason.*, vol. SU-27, pp. 360-369, Nov. 1980.
- [14] B. Widrow *et al.*, "Stationary and nonstationary learning characteristics of the LMS adaptive filter," *Proc. IEEE*, vol. 64, pp. 1151-1162, 1976.
- [15] B. Widrow and J. M. McCool, "A comparison of adaptive algorithms based on the methods of steepest descent and random search," *IEEE Trans. Antennas Propagat.*, vol. AP-24, pp. 616-637, 1976.
- [16] J. E. Bowers, B. T. Khuri-Yakub, and G. S. Kino, "Broadband efficient thin film Sezawa wave interdigital transducers," *Appl. Phys. Lett.*, vol. 36, pp. 806-807, 1980.

# Surface-Acoustic-Wave Random-Access Memories

GIANFRANCO F. MANES

**Abstract**—An acoustic tapped-delay line (TDL) undermultiplexer control exhibits random-access-memory (RAM) capability; programmable time compression/expansion is achieved by controlling the difference between tap switching interval and intertap delay. A serial-in/parallel-out configuration can perform spectral compression of high input bandwidths, while requiring a single sampling operation to be performed, at the output data rate; dual properties are demonstrated by a parallel-in/serial-out organized RAM used for time compression. A new powerful  $N$ -phase configuration is discussed, which allows the intrinsic switching capability of multiplexers employed to be increased by  $N$ , while offering high dynamic range capability.

The basic operation of the new technique is discussed, some theoretical aspects are investigated, and various effective configurations are described. In particular, the natural format of the time contracted/segmented output from a nonlinear convolver, asynchronously operated, is recovered; a clock-programmable bandpass filter is demonstrated, based on complementary time compression expansion. Extension to read-only memory (ROM) is briefly outlined, with reference to frequency synthesis.

Finally, processing of signals in baseband format is demonstrated using acoustic TDL's, via a simple modulation technique, which increases flexibility and the potential attraction of the new technique.

## I. INTRODUCTION

**S**URFACE-ACOUSTIC-WAVE (SAW) tapped-delay lines (TDL) have represented the first attractive implementation of analog transversal structures, operating in the intermediate frequency range, providing almost ideal time-domain discrete access, and offering unique signal-

processing capabilities in terms of maximum equivalent sampling rate and  $BT$  product. The advent of charge-transfer devices (CTD) has more recently permitted the realization of analog integrated transversal structures in the complementary baseband frequency range. CTD's, where data samples are stored in the form of charge packets and transferred in clocked shift-register fashion, exhibit random-access-memory (RAM) operation capability, thus forming an ideal candidate for applications requiring programmability at clock rates not exceeding a few megahertz. Conversely, surface-acoustic-wave (SAW) devices, where data are transferred in the form of a fixed-velocity piezoelectric wave and collected by a rigid tapping structure, appear inherently prevented from application to the important class of programmable signal-processing operations. A relative degree of programmability has been so far achieved only by special SAW devices, based on nonlinear interaction of acoustic waves in the piezoelectric substrate [1] or in coupled diode arrays [2] or in doped semiconductors [1].

The inherent limitations associated with the rigid time-access structure of SAW TDL's can be circumvented, however, by a recently demonstrated technique [3], [4] basically consisting in demultiplexing the parallel available data at a programmable rate through an analog multiplexer. The technique results in a SAW-based RAM, exhibiting clock-programmable time-compression/expansion and time-delay capability, relying on the particular sampling operation involved rather than on a new physical mechanism.

A number of unique configurations based on this tech-

Manuscript received May 1, 1980. This work was supported under contract with the special project on Biomedical Technologies of the National Research Council.

The author is with Istituto di Elettronica, Università di Firenze, Florence, Italy.

nique are described in this paper, which allow signal-processing operations previously restricted to CTD's to be performed using SAW-based devices. Novel applications have been envisaged. Serial-in/parallel-out configurations of SAW RAM's are described, offering unique capabilities for time expansion/compression. A powerful  $N$ -phase structure is introduced, which allows clock frequencies to be achieved  $N$  times higher than those obtainable by a single multiplexer, and the device performance to be greatly improved.

A SAW RAM operated in the time-expansion mode is demonstrated capable of recovering the natural format of the time-segmented and contracted output from an asynchronously operated nonlinear convolver. A variable-bandpass filter, whose bandwidth is controlled by the clock of time-expansion/compression units, is demonstrated.

A SAW RAM can be converted into a read-only memory (ROM), which permits permanent storage of analog sinusoidal samples [5] at the individual outputs, resulting in sine-cosine look-up tables for programmable discrete frequency synthesis. SAW RAM's can process baseband signals, made compatible with the SAW bandpass frequency response via a suppressed-carrier modulation process. The RF carrier is, however, ignored in the processing, as the intertap delay is made equal to an integer number of carrier cycles. Alternatively, a simple technique based on a classical amplitude modulation-demodulation process [6] can provide compatibility of SAW TDL bandpass frequency response with baseband data format.

## II. SAW RANDOM-ACCESS MEMORY

### A. Basic Operation

In Fig. 1(a), a realization of the SAW RAM is shown, consisting of an  $N$ -tap TDL, whose taps are individually controlled by an analog multiplexer, operated at a clock rate  $f_c = 1/T_c$ , from 1 to  $N$  and vice versa, depending on the up/down mode control [3]. The input waveform is applied to the acoustic port and the multiplexer common node represents the output, the configuration operating in a serial-in/parallel-out mode. As mentioned above, the intertap delay  $T_p$  is required to be an integral multiple of the SAW synchronous frequency  $f_0$ , so ensuring phase coherence of the individual outputs and allowing baseband format of the output sampled sequence to be recovered by synchronous demodulation.

As the individual taps are scanned at the clock interval  $T_c$  from  $N$  to 1, a readout sequence of  $N$  natural samples, contiguously positioned, appears at the multiplexer output; however, owing to the TDL temporary data storage capability, a fixed time difference  $T_p$  exists between the readout interval  $T_c$  and the equivalent sampling interval  $T_c + T_p$ . During each readout cycle, a segment of duration  $N(T_p + T_c)$  is processed, resulting in an output sequence of natural samples

$$\sum_{k=1}^N a(t - kT_p) p(t + kT_c) \quad (1)$$

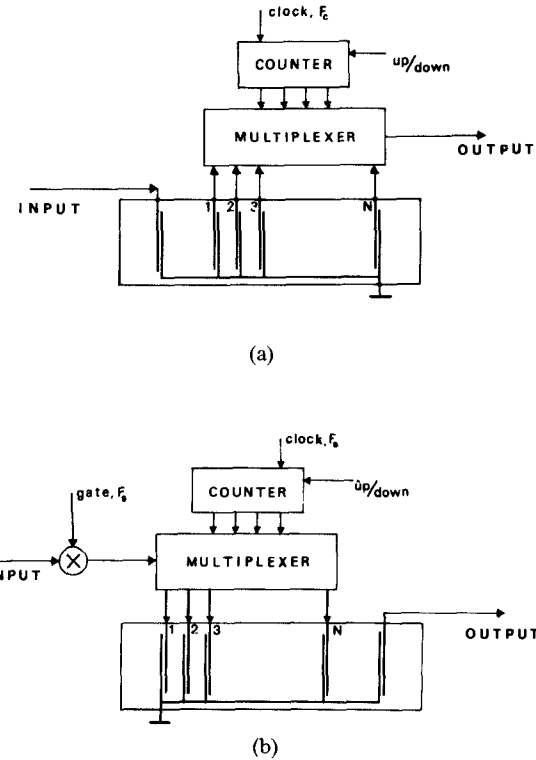


Fig. 1. SAW RAM schematic diagram.

where  $a(t)$  is the input waveform and  $p(t)$  is a pulse of duration  $T_p$ . The time compression factor

$$s_c = \frac{T_c + T_p}{T_c} \quad (2)$$

equals the ratio between the readout rate and the sampling rate. Very attractive features are envisaged when the device is operated in the up mode. As the taps are sequentially accessed from 1 to  $N$ , in fact, owing to TDL discrete-time-access capability, individual samples of the input waveform are read out at an equivalent sampling interval ( $T_c - T_p$ ) equal to the difference between multiplexer clock interval  $T_c$  and the acoustic sampling interval  $T_p$ . The resulting time expansion factor is

$$s_e = \frac{T_c - T_p}{T_c}. \quad (3)$$

By increasing sampling rates, correspondingly increased processable bandwidths can be achieved as the readout interval approaches  $T_p$ . Thus the device, directly operating on data available in analog format, where the sampling rate is dynamically determined by the readout clock itself, exhibits the unique capability of allowing spectral compression of high input bandwidths  $B$  to be attained, while requiring one single sampling operation to be performed at the output bandwidth rate  $2Bs_e$ , provided the tap bandwidth is consistent with the information being processed.

It should be noted, in addition, that this technique results in decreasing output bandwidths being obtained, with correspondingly increasing clock rates, unlike sampled-data devices, where a rigid ratio relates data and

clock rates. Programmable time expansion can then be performed, over a wide range, without necessarily requiring variable low-pass filtering to be provided, for signal reconstruction.

An alternative implementation of the SAW RAM is shown schematically in Fig. 1(b), resulting in a parallel-in/serial-out configuration, exhibiting dual behavior, with respect to the one previously described, when used in the time compression mode; the related discussion will then be restricted to this latter case. With reference to Fig. 1(b), the individual taps are now scanned from 1 to  $N$  at a suitable clock interval  $T_s$ , but each sample of the input waveform is read in during a portion  $T_c \leq (T_s - T_p)$ , according to the operation of the serial sampling gate, appearing in Fig. 1(b). The following sample, of the same duration and spaced by a dead time  $T_p$  with respect to the previous one, is then read in at the subsequent tap, and so on. As a result, a sequence of natural samples (1) of duration  $T_c$  and contiguously positioned, is obtained at the output, as the dead time intervals are exactly compensated for by the acoustic delay  $T_p$ . A time compression factor is obtained, identical with that expressed by (2), as the ratio between sampling rate  $T_c + T_p$  and readout rate  $T_c$ . It should be noted, however, that owing to the intrinsic TDL data memory capability, where natural samples can be stored at a tap for a time  $T_p$ , before appearing at a subsequent tap, the actual readout interval is determined by the difference between the multiplexer clock interval itself and the acoustic delay  $T_p$ . Dual properties are obtained, as mentioned above, i.e., increasing readout rates, corresponding to increasing time compression, can be achieved as  $T_s$  approaches  $T_p$ . Thus the device exhibits the attractive feature of allowing compression in short time slots to be achieved, while requiring one single sampling operation at the input bandwidth rate. However, in this case, a tap bandwidth consistent with that of the processed information is required.

In the above discussion, the device operation has been interpreted under the heuristic assumption of a straightforward analogy with sampled-data devices where the information can be temporarily stored in the form of instantaneous samples; with the described technique, however, the information is handled in the form of natural samples and no physical data storage is allowed for in the TDL structure itself.

In order to gain an insight into the basic device operation, the spectral structure of the sample sequence (1) was investigated; in the Appendix, a mathematical derivation is given, whose conclusions are briefly summarized here. According to (A5), (1) can be interpreted as a sequence of instantaneous samples of the input waveform  $a(t)$  at a sampling interval  $|T_c \pm T_p|$ , depending on the operation mode, whose time base is modified according to the desired factor  $s$ ; the instantaneous sample sequence is then convoluted with the special function  $w(t)$ , whose spectral response is shown in Fig. 12 with nulls at the clock frequency harmonics.

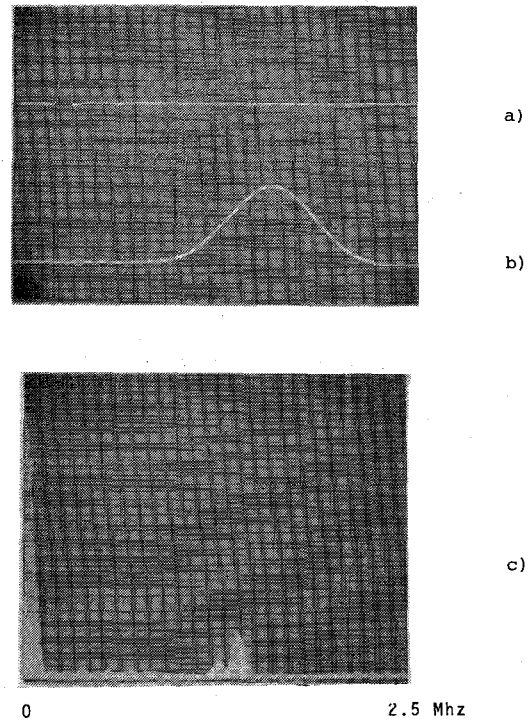


Fig. 2. Time-expansion experiment using a serial-in/parallel-out RAM.

The operation sequence identified by (A5) is recognized as being formally identical with that performed by sampled-data memories, where  $w(t)$  is replaced by a sampling and holding, providing on the other hand a spectral weighting very similar to  $W(f)$ . The analysis performed thus confirms the close analogy between SAW RAM's and sampled-data devices, although based on very different physical operation mechanisms. The programmable data-transfer capability resulting from clocked data-shifting is replaced here by the accessing control of the individual TDL taps, performing the function of analog memory cells; this results in a natural rather than an instantaneous output format, while, however, retaining the same information content.

### B. Experimental Results

The signal-processing capability of the two configurations described is demonstrated, using SAW RAM's implemented as hybrid circuits containing both TDL and switching circuitry, and assembled using a chip-and-wire technique. First, time expansion was performed using a 32-cell RAM with 350-ns acoustic delay and 4-MHz tap bandwidth. A first experiment is shown in Fig. 2; a triangular waveform of approximately 800-ns duration, with significant spectral components up to some megahertz represents the input signal, and it is shown in Fig. 2, trace (a), at a 2-μs/div time base. After suppressed-carrier modulation, the signal was fed to the device, operating in a serial-in/parallel-out configuration at a clock frequency of approximately 2.65 MHz, resulting in a time expansion factor of 12.5. The readout sampled sequence was coherently

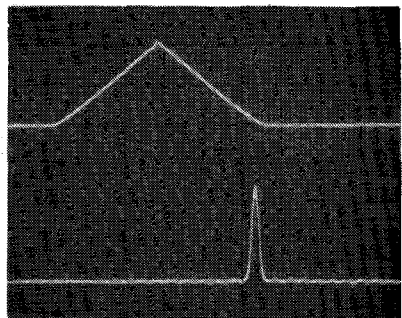


Fig. 3. Time compression experiment using a parallel-in/serial-out RAM.

demodulated and low-pass filtered at 1-MHz cutoff frequency with 48-dB/octave rolloff. The filtered signal is displayed in trace *b* of Fig. 2, with the same 2- $\mu$ s/div time base as before.

A spectrum analyzer display of the expanded output, prior to filtering, is shown in trace *c*, in the frequency range 0–5 MHz, with 500-kHz/div horizontal scale and linear vertical scale. The weighted harmonic sideband is identified around the readout clock frequency of 2.65 MHz, with the particular shape resulting from the discussed sampling operation. The compressed spectrum exhibits a 100-kHz–6-dB bandwidth against the 1.25-MHz–6-dB bandwidth of the input triangular waveform, according to the expansion factor obtained. The equivalent input sampling rate is 33 MHz, under the described operative conditions, resulting from the difference between clock interval, 380 ns, and acoustic delay, 350 ns. Accordingly, the processable input bandwidth is 16.5 MHz, corresponding to an output bandwidth of 1.325 MHz and equals to one half the readout clock frequency. With the device used, however, the processable bandwidth was limited by the 15-percent tap fractional bandwidth.

For time compression experiments, a 16-cell 700-ns acoustic-delay SAW RAM was used. A triangular waveform compressed by a factor of 10 is shown in Fig. 3 at 2  $\mu$ s/div. Readin frequency, equal to the multiplexer clock frequency, was 1.28 MHz, while the equivalent readout rate was as high as 12.5 MHz, as determined by the difference between clock interval, 780 ns, and the acoustic delay.

### III. MULTIPHASE CONFIGURATION

Possible limitations of the device performance are related to the external multiplexer used for tap access control. When using CMOS integrated multiplexers with binary address control and on-chip decoding, maximum clock frequency is limited to a few megahertz, while switching transient noise at these frequencies severely limits the dynamic range capability. Switching noise gives rise to frequency spikes mainly concentrated at the harmonics of the clock frequency. As the device is operated at RF, some of these frequency spikes can occur in the useful band, thus preventing their removal by filtering out.

An alternative configuration, referred to as "multiphase,"

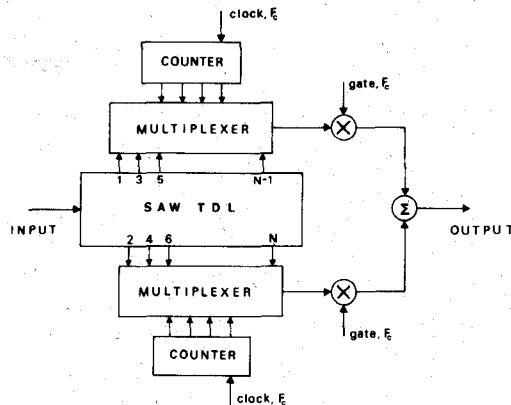


Fig. 4. Two-phase SAW RAM configuration.

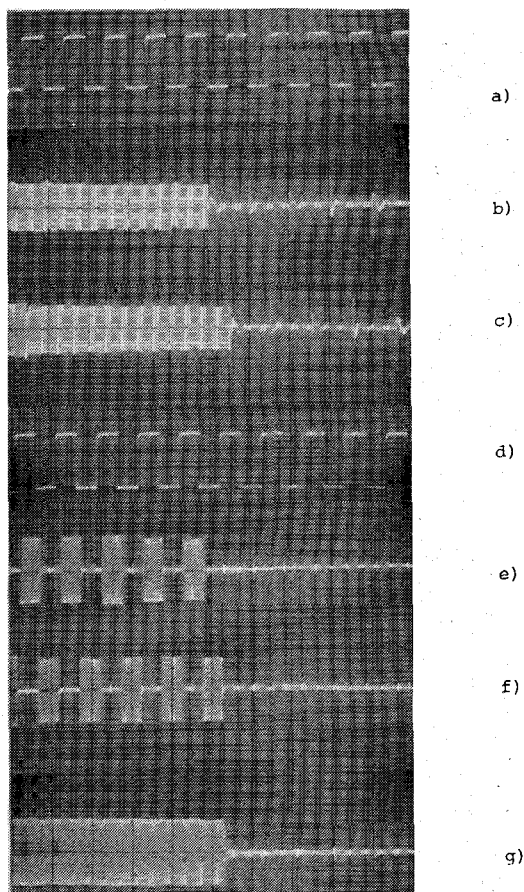


Fig. 5. Two-phase SAW RAM experiments.

has been conceived, that allows both a dramatic reduction of the switching noise and an increase in maximum clock frequency capability. This configuration is described with reference to Fig. 4, where a two-phase architecture is shown. The arrays of even- and odd-numbered taps of the SAW TDL are each independently controlled by a multiplexer having  $N/2$  gates; the binary addresses of the two multiplexers are provided by an even and an odd clock waveform, respectively, at the same rate  $F_c$ , but operated in phase opposition.

In Fig. 5, trace *a*, the even clock waveform with  $F_c$

approximately 500 kHz is shown at 2  $\mu$ s/div. The even and odd sample sequences obtained at the multiplexer outputs are displayed in traces *b* and *c*, respectively; switching transients, occurring at the clock trailing edges, are clearly observable. As the even and odd sampling intervals overlap, however, two external analog gates with 50-percent duty cycle and driven by the same clock frequency are connected at the multiplexer outputs. In this manner, as only one half of the sampling interval is transmitted through the analog gates, the switching transients are suppressed simply by shifting each sampling wave by a quarter of a period with respect to the corresponding clock. Thus sequences of even and odd samples turn out interleaved, and, after summation, the output data rate results in a two-fold clock rate,  $F_c$ , of each individual multiplexer. Trace *d* in Fig. 5 shows the even gating waveform, while the odd one is simply negated; traces *e* and *f* show the sampled sequences as appearing after gating, exhibiting switching transients suppressed to a large extent; and finally trace *g* shows the 1-MHz rate samples sequence resulting after summation. The two-phase configuration implemented using CMOS multiplexers and external double-balanced mixers as sampling gates, could be operated up to 10 MHz, with noise suppression in excess of 40 dB at 9-MHz clock and 55 dB at 1-MHz clock.

The extension of the above technique to an  $M$ -phase configuration, employing  $M$  multiplexers and  $M$  external sampling gates, appears quite straightforward. It is worthwhile emphasising that the output data rate would be  $M$  times higher than the clock frequency of each individual multiplexer, thus allowing very high data rates to be achieved.

#### IV. LARGE $BT$ PRODUCT ARCHITECTURES

The signal-processing capability of the SAW RAM in terms of  $BT$  product equals the number of processable samples during the same readin or readout cycle and, thus the tap count.  $BT$  products of the order of hundreds, then, require a high tap count, resulting in a number of undesirable effects, e.g., multipath reflections in the tapping structure and crosstalk. A possible means of circumventing these limitations is represented by the configuration shown in Fig. 6, already discussed elsewhere [3]. The configuration basically consists of a serial-in/parallel-out RAM, with a multiple-output capability, i.e., a lower density tapping structure, also controlled by a demultiplexer. Only the operation in the time compression mode is considered; the readin structure is continuously and repetitively operated from 1 to  $N$  at a suitable clock rate  $F_s$ , with external gate duration  $T_c$ , similarly to the one discussed above. Each readin cycle gives rise to a sequence of  $N$  samples of duration  $T_c$  to be propagated towards the output structure with a dead time  $NT_p$  between any two subsequent sequences. The output demultiplexer is operated from  $M$  to 1 at the readout cycle  $N(T_s - T_p)$ , synchronously with the readin operation, in such a manner that each readout cycle

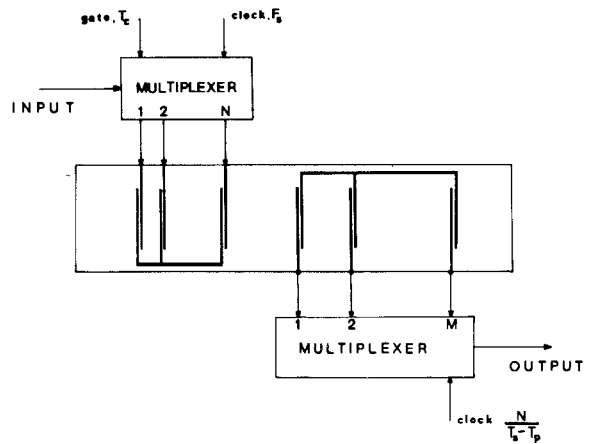


Fig. 6. Large  $BT$  product architecture.

starts exactly as a readin sequence begins being available at the corresponding tap. Subsequent readin sequences are then read out at the subsequent output taps; as the output intertap delay  $NT_p$  exactly equals the intersequence dead-time interval, the individual sequences are properly contiguously positioned and, after an overall readout cycle, a total number of  $N \times M$  samples are obtained, in the proper format, while controlling only  $(N+M)$  taps. A dual operation is performed when input and output are interchanged; with reference to the time expansion case, the input waveform is now fed to the lower density structure, being now scanned in sequence from 1 to  $M$  at the same clock interval  $N(T_s - T_p)$  as before. Each readin segment is processed by the output structure, operating in a parallel-in/serial-out organization, for a total time interval  $NT_s$  as imposed by the required expansion factor. The subsequent readin segments are, however, spaced by dead-time intervals  $NT_p$ , due to the input multiplexing, and again in this case proper interleaving is obtained.

Both compression as well as expansion can then be achieved, using a more efficient RAM configuration, while considerably reducing the required tap count.

#### VI. TIME BASE RECOVERING IN NONLINEAR CONVOLVERS

The particular dynamic memory capability of the described device can be employed for real-time reconstruction of the correct format of the contracted-in-time and segmented output from an asynchronously operated SAW nonlinear convolver. It is known that in SAW convolvers convolution between a signal and a reference, propagated along opposite directions, is obtained only if nonlinear interaction occurs completely in a limited region between the input transducers, the output resulting contracted-in-time by a factor of two. Morgan *et al.* [7] have demonstrated that asynchronous operation can be achieved for arbitrary signal delay, provided that the reference waveform is made repetitive, and the convolver output is gated with the same repetition ratio and one-to-one mark-to-space ratio. The convolver output appears segmented in a series

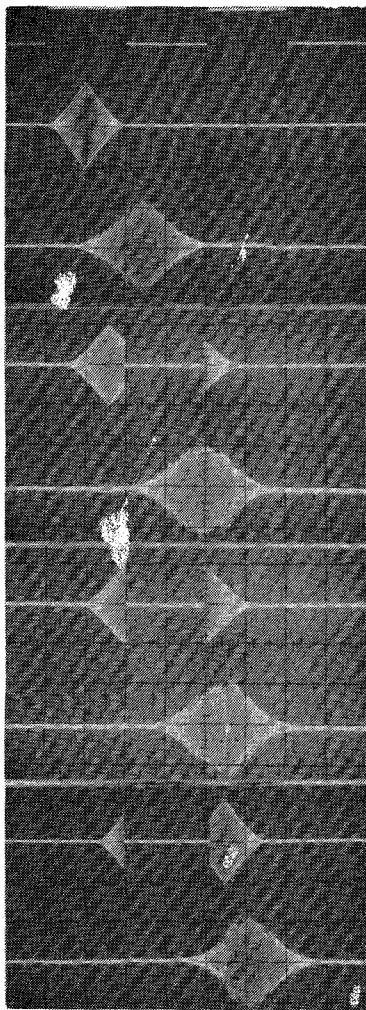


Fig. 7. Time base recovering in a nonlinear convolver.

of time slots alternating with dead spaces, the segmentation corresponding to the gate action. The natural format and time base of this output can be recovered using a SAW RAM, operated in time-expansion mode with  $T_c = 2T_p$ , yielding an expansion factor of 2, and a readout cycle  $N(T_c - T_p) = NT_p$  equal to the slot duration. The device must be continuously and repetitively operated from 1 to  $N$ , synchronously with the convolver gate, so that each individual slot is processed in a readout cycle.

The segmented output from an asynchronously operated convolver was simulated by periodically gating a triangular waveform, representing the convolution of two rectangular pulses. Altering the delay between the triangle and the gate results in a different segmentation of the simulated convolver output. Three different situations are represented in Fig. 7, where the capability of the TE unit to recover the natural format of the triangular waveform is demonstrated for all cases. The clock frequency was 1.415 MHz, so that the dead spaces are compensated for by the device storage time  $NT_p$ , and a time expansion of two, the recovery of the original time base of the convolver input was obtained. It is known that in a real situation the convolver output suffers

a delay equal to one half the delay in arrival time of the input signal.

It is to be noted that the TE unit recovers the original delay as well, as it appears from Fig. 7, where the relative delay of the reconstructed outputs is twice the relative delay of the simulated convolver outputs.

## VII. CLOCK-PROGRAMMABLE BANDPASS FILTER

A bandpass filtering architecture, where the filter bandwidth is controlled by the clock frequency of associated complementary TE and TC units, has been conceived.

The input waveform is fed to the TC unit, having  $N$  taps and operated at a clock rate  $F_c$ . At each readout cycle, a segment of duration  $N(T_p + T_c)$  of the input waveform is compressed into a sample sequence of duration  $NT_c$ , and applied to a cascaded fixed-bandpass filter. Let  $g_s(t/s)$  be the compressed sampled signal,  $s$  the compression ratio, and  $h(t)$  the filter impulse response. The filter output, described by

$$g_s(t/s) \times h(t) \quad (4)$$

is applied to the TE unit, having  $N+M$  taps and operated at the clock rate  $F'_c = F_c/s$ , so as to provide an expansion factor  $1/s$ . The TE unit samples the input (4) at time intervals  $T'_c - T_p = T_c$ , thus processing a time duration  $(N+M)T_c$  for each scanning cycle. A suitable increase in tap count  $M$ , with respect to that of the TC unit  $N$ , is required in order completely to process the filter output (4), which exceeds  $NT_c$  by the duration of the filter impulse response. After proper interpolation filtering, the final output results in

$$u(t) = g(t) \times h(st) \quad (5)$$

i.e., everything goes as if the filter bandwidth were compressed by the factor  $s$ , controlled by the clock rate. A complete architecture of the system, allowing for asynchronous processing of signals of arbitrary duration, is shown in Fig. 8. The TC unit is periodically operated every  $NT_p$  seconds, so that the input signal is compressed into time slots of width  $NT_c$  interleaved with dead intervals of width  $NT_p$ . The TE unit is subdivided into two adjacent sections, one consisting of  $N$ , the second of  $M$  taps, each controlled by a multiplexer. The first  $N$ -tap section is continuously and repetitively operated, while the second  $M$ -tap section is operated at the end of each cycle of the first one. In this way, correct superposition of the processed signal segments from the bandpass filter is ensured. Experimental demonstrations of a clock-controlled variable bandpass filter are given in Fig. 9. The filter was a double-tuned resonant circuit centered on the 17-MHz SAW synchronous frequency with 1.2-MHz -3-dB bandwidth. Its amplitude spectrum, displayed at the top of Fig. 9, appears compressed by a factor of 2 in the middle trace, when operating the TC unit at 2.9 MHz and the TE unit at 1.45 MHz; compression by 5 is shown in the bottom photograph, obtained with clock frequencies of 11.6 MHz for compression and 2.3 MHz for expansion. The TC unit was a

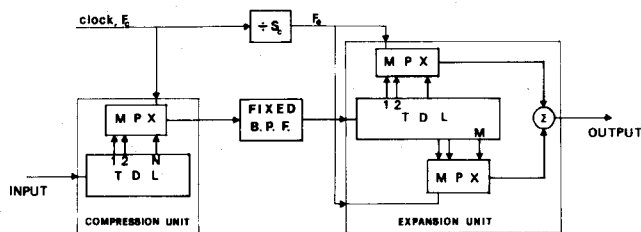


Fig. 8. Clock-programmable bandpass filter architecture.

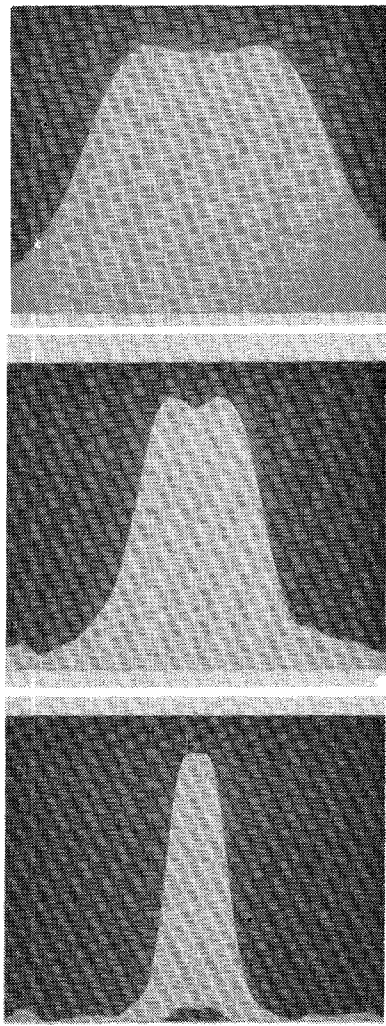


Fig. 9. Clock-programmable bandpass filter experiments.

serial-in/parallel-out SAW RAM, and the TE was a two-phase SAW RAM, both with 350-ns acoustic delay.

### VIII. SAW ROM FOR DISCRETE FREQUENCY SYNTHESIS

A SAW RAM can be converted into an analog ROM capable of discrete frequency synthesis. The configuration, described elsewhere [4], consists of applying to the acoustic port of a SAW RAM a CW waveform, whose frequency exceeds the SAW synchronous frequency by the amount

$F = 1/NT_p$ , and of coherently demodulating the outputs. After low-pass filtering, analog sinusoidal samples  $\cos(2\pi k/N)$ , where  $k = 1, \dots, N$ , result permanently stored at the TDL outputs. An indefinite sequence of sinusoidal samples are read out by sequentially and repetitively operating the multiplexer at a clock frequency  $F_c$ , thus generating an oscillation of frequency  $f_1 = F_c/N$ . By activating the multiplexer gates in increments of  $m$ , the stored samples are also accessed in increments of  $m$ , thus generating the  $m$ th harmonic of the lower oscillation. As the sampling frequency  $F_c$  allows a maximum frequency  $F_c/2$  to be generated, the number of harmonics does not exceed  $N/2$ . This operation is strictly parallel to the operation of a digital frequency synthesizer, employing digital ROM's for the implementation of sine-cosine look-up tables, introduced by Tierney *et al.* [8].

### IX. SAW BASEBAND PROGRAMMABLE FILTERS

CTD programmable transversal filters, where the weights synthesizing the required response are set by multiplying digital-analog (MDA) convertors, have been extensively developed [9], [10]. Similar configurations cannot be directly implemented using SAW TDL's, as the RF format of the outputs from the taps prevents the use of baseband-operating arithmetic units for weight control. The technique of coherently demodulating the signal from each tap, so as to recover the baseband format, even though possible in principle, is not attractive because of the complex hardware required.

A novel approach has been introduced [5] which permits the coupling of baseband signals at the taps output, using significantly simpler hardware. By this technique, SAW transversal structures can be used as building block of programmable filters analogous to the CTD-based MDA-controlled programmable filters.

The new approach simply relies on a classical amplitude modulation-demodulation process. The input signal is impressed as instantaneous amplitude variation of a carrier of frequency  $f_0$  equal to SAW synchronous frequency, while the baseband format of the delayed output at each tap is recovered through a nonlinear detection circuit. The interface circuitry, Fig. 10, is extremely simple. The baseband input  $s(t)$  is applied to one gate of a dual-gate MOSFET, the carrier oscillation being applied to the second gate. The drain load is constituted by the SAW input transducer, including a shunt tuning coil. The individual outputs are then amplitude detected before processing. A number of baseband compatible SAW filters have been realized using external adjustable resistors to control the desired tap-weighting configuration. The building block was a 16-tap 17-MHz synchronous-frequency SAW delay line, with peak detection circuitry implemented in hybrid form. The inter-tap delay was 570 ns, corresponding to 1.7-MHz sampling rate capability.

Experiments of low-pass filtering and of matched filtering of a 7-bit Barber code have been previously presented.

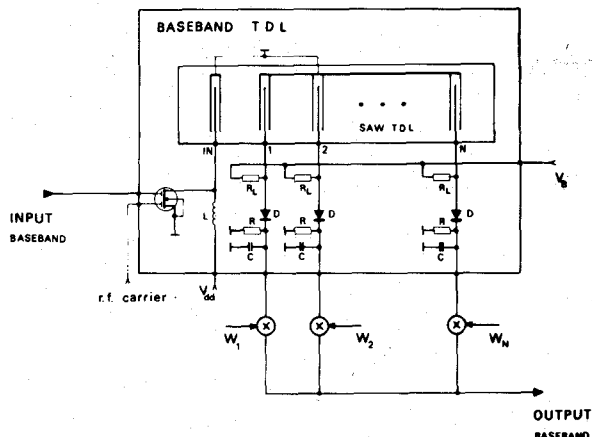


Fig. 10. Baseband SAW TDL schematic diagram.

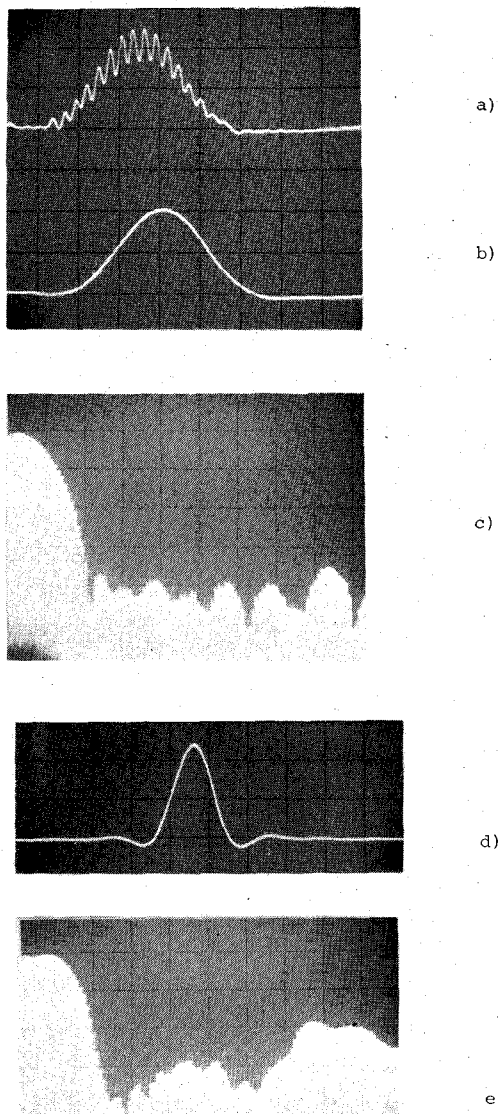


Fig. 11. Baseband transversal filter experiments.

Additional experiments are displayed in Fig. 11; trace *a* shows the sampled impulse response of a 200-kHz 3-dB bandwidth Hamming window; trace *b* shows the corresponding continuous response, obtained after interpolation using an 800-kHz cutoff 24-dB/octave rolloff low-pass filter; in trace *c* is displayed the device frequency response in the range 0–2 MHz, exhibiting sidelobe suppression close to the theoretical –40-dB level. The continuous impulse response obtained by shaping the tap weights configuration according to a Hamming-weighted  $\sin x/x$  profile is shown in trace *d*, while trace *e* shows the frequency response exhibiting a 300-kHz–3-dB bandwidth low-pass characteristic with fairly good in-band ripples behavior, and the first harmonic at 1.7 MHz, 20 dB down with respect to the main response; –30-dB sidelobes appearing between 800 kHz and 1.2 MHz are attributed to aliasing effects.

## X. CONCLUSIONS

A novel technique has been described, which allows SAW devices to operate in areas and at frequency ranges previously restricted to analog or digital sampled-data devices. Based on a new concept of dynamic memory, the technique allows data storage and rate conversion to be achieved, while requiring a single sampling operation; two alternative SAW RAM configurations have been discussed, exhibiting dual properties for time compression/expansion. Experiments have been described which demonstrate the attainment of high data rates, with correspondingly lower tap switching frequency. Time expansion by 15, with equivalent input 33-MHz sampling rate, and time compression by 10, with 13-MHz output data rate, have been obtained, by using 2.65- and 1.325-MHz clock rates, respectively. Switching noise, a potential limiting factor, can to a large extent be reduced by using gating techniques, which are also desirable for increasing tap switching frequency, when employed in an *N*-phase configuration. Particular configurations have also been described, capable of providing large *BT* product, while controlling a reasonably limited tap count. Finally, a new technique has been demonstrated which permits very easy compatibility of SAW TDL's with baseband data domain, thus allowing the new technique to be implemented at either RF or baseband, while preserving the attractive features of SAW devices.

## APPENDIX

Frequency-domain analysis of the sample sequence (1), in the text, is performed by taking the convolution

$$\sum_{n=-\infty}^{\infty} \int A(\Omega) \exp(-jn\Omega T_p) P(\omega - \Omega) \cdot \exp\{j(\omega - \Omega)nT_c\} d\Omega \quad (A1)$$

where  $A(\omega)$  and  $P(\omega)$  are the spectra of the input waveform  $a(t)$  and sampling pulse  $p(t)$ , respectively. By recal-

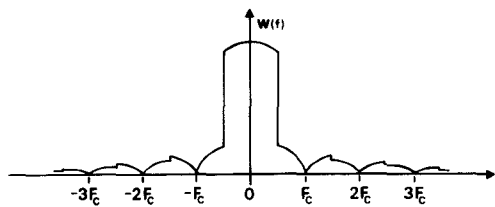


Fig. 12.

ling the following:

$$\sum_{n=-\infty}^{\infty} \exp(jn\omega T) = \sum_{k=-\infty}^{\infty} \delta\left(\omega - \frac{2\pi k}{T}\right). \quad (A2)$$

Equation (2) can be rearranged as

$$\int A(\Omega)P(\omega - \Omega) \sum_{k=-\infty}^{\infty} \delta\left(s_c\Omega - \omega \frac{2\pi k}{T_c}\right) d\Omega \quad (A3)$$

where  $s_c$  is the time compression factor defined by (2) in the text. Inspection of (A3) allows the desired spectral expression to be obtained

$$\sum_{k=-\infty}^{\infty} A\left(\frac{\omega}{s_c} - \frac{2\pi k}{T_p + T_c}\right) P\left(\omega \frac{T_p}{T_p + T_c} + \frac{2\pi k}{T_p + T_c}\right). \quad (A4)$$

Provided  $a(t)$  is a band-limited signal, as required by the sampling operation, the terms  $P(\omega)$  in (A4) result in a weighting function  $W(f)$  similar to that drawn in Fig. 1(a), having nulls at the harmonics of clock frequency  $F_c$ , and independent of the particular signal being processed (see Fig. 12).

Equation (A4) can be then inverse transformed giving an equivalent expansion of the sampled sequence (1)

$$w(t) \times \left\{ \sum_{k=-\infty}^{\infty} a(s_c t) \delta\left(t - k \frac{T_p}{T_p + T_c}\right) \right\} \quad (A5)$$

where  $w(t)$  is the inverse Fourier transform of  $W(f)$ . Similar results can be derived for the cases of time expansion/reversal.

#### ACKNOWLEDGMENT

The author wishes to thank Dr. C. Atzeni, IROE-CNR, for many helpful discussions and suggestions. Technical support by C. Raffini and P. Tortoli is also gratefully acknowledged. The SAW devices and hybrid circuits used for the experiments were made and assembled at the Laboratorio di Microelettronica, Elettronica spa, Rome, Italy, Dr. S. Gasperini responsible.

#### REFERENCES

- [1] G. S. Kino, "Acoustoelectric interactions in acoustic-surface-wave devices" (Invited Paper), *Proc. IEEE*, vol. 64, no. 5, pp. 724-748, May 1976.
- [2] T. M. Reeder and M. Gilden, "Convolution and correlation by non-linear interaction in a diode-coupled delay line," *App. Phys. Lett.*, vol. 22, no. 1, pp. 8-10, Jan. 1973.
- [3] G. F. Manes, "Experiments on variable delay and time base variation using a programmable SAW device," in *1977 IEEE Ultrasonics Symp. Proc. IEEE Cat. No. CH 1264-1SU*, pp. 619-622.
- [4] ———, "A novel surface-acoustic-wave device for electronically variable delay," *Proc. IEEE (Lett.)*, vol. 66, no. 4, pp. 519-520, Apr. 1978.
- [5] G. F. Manes and C. Atzeni, "Discrete frequency synthesis using an analogue ROM," *Electron. Lett.*, vol. 15, no. 12, pp. 350-352, June 1979.
- [6] ———, "Baseband compatible SAW processors," *Electron. Lett.*, vol. 15, no. 20, pp. 661-662, Sept. 1979.
- [7] D. P. Morgan, J. H. Collins, and J. G. Sutherland, "Asynchronous operation of acoustic wave convolvers," in *1972 IEEE Ultrasonics Symp. Proc. IEEE Cat. No. CHO 708-8SU*, pp. 296-298.
- [8] J. Tierney, C. M. Rader, and B. Gold, "A digital frequency synthesizer," *IEEE Trans. Audio Electroacoust.*, vol. AU-19, pp. 48-57, Mar. 1971.
- [9] D. F. Barbe, D. W. Baker, and K. L. Davies, "Signal processing with CCD's," *IEEE J. Solid-State Circuits*, vol. SC-13, June 1978.
- [10] J. E. Dilley, M. Naughton, R. C. S. Morling, G. D. Cain, and A. H. Abed, "A microcomputer-controlled adaptive CCD transversal filter," in *Proc. 3rd CCD Int. Conf. (Edinburgh, Scotland, 1976)*, pp. 269-276.